Epoxy-cross-linked Polyamine CO2 Sorbents Enhanced via Hydrophobic Functionalization

Journal:	*Chemistry of Materials*
Manuscript ID	cm-2019-00574j.R2
Manuscript Type:	Article
Date Submitted by the Author:	29-May-2019
Complete List of Authors:	Hamdy, Louise; Swansea University, Department of Engineering Wakeham, Russell; Swansea University Taddei, Marco; Swansea University, Energy Safety Research Institute Barron, Andrew; Swansea University, ESRI Andreoli, Enrico; Swansea University,

Epoxy-cross-linked Polyamine CO_2 Sorbents Enhanced via Hydrophobic Functionalization

Louise B. Hamdy,† Russell J. Wakeham,† Marco Taddei,† Andrew R. Barron,†‡ Enrico Andreoli†*

†Energy Safety Research Institute, Swansea University, Bay Campus, Swansea, SA1 8EN, United Kingdom

‡Department of Chemistry and Department of Materials Science and Nanoengineering, Rice University, Houston, Texas 77005, United States

ABSTRACT: Optimizing sorption capacity and amine efficiency are among the major challenges in developing solid carbon dioxide sorbents. Such materials frequently feature polyamines impregnated onto supports adding weight to the sorbents. This work presents the cross-linking of polyethyleneimine (PEI) by the industrially available epoxy resin, bisphenol-A diglycidyl ether (DER) to form support-free sorbent materials. Prior to cross-linking, the polyamine chain is functionalized with hydrophobic additives; one material modified with the branched chain hydrocarbon 2-ethylhexyl glycidyl ether displays CO_2 uptake of 0.195 g/g, 4.43 mmol CO_2/g (1 atm single component CO_2, 90 °C). The additive loading affects the cross-linking, with the lesser cross-linked materials showing more favorable sorption capacities and higher amine efficiencies. The type of additive also influences sorption, with the larger, longer and bulkier additives better able to free the amine from their hydrogen bonding network, generally promoting better sorption. As well as increasing CO_2 uptake, the additives also reduce the optimum sorption temperature, offering a handle to tune sorbents for specific working conditions. The best performing material shows high selectivity for CO_2 sorption, and under sorption cycles in a 10% CO_2/90% N_2 mixture, utilizing temperature swing desorption, demonstrates a good working capacity of 9.5% CO_2 uptake over the course of 29 cycles. Furthermore, humidity has been found to promote CO_2 sorption at lower temperatures with a CO_2 uptake of 0.235 g/g, 5.34 mmol/g (1 atm single component CO_2, 25 °C) using a pre-hydrated sample. Overall, these findings confirm the value of our approach where cross-linking emerges as a valid and practical alternative to loading polyamines onto solid supports. This work demonstrates the versatility of these types of materials and their potential for use in large scale carbon capture systems.

INTRODUCTION

Atmospheric CO_2 levels continue to rise, with global anthropogenic emissions from both the burning of fossil fuels and cement production projected to increase to 43.2 Gt CO_2 yr^{-1} in 2019.[1] To abate this rise and the associated environmental impacts, there is a strong focus within the scientific community to develop materials capable of capturing CO_2 from power and industrial flue gas mixtures with the purpose of sequestering or utilizing the absorbate.

Amine based organic compounds have attracted much interest as CO_2 absorbents due to their reversible reaction to form carbamate and/or carbonate and bicarbonate species, depending on the amine and conditions of absorption.[2-5] The absorption of CO_2 from aqueous amine solutions is the most advanced technology for large scale CO_2 capture,[6] however drawbacks include the high regeneration costs and corrosion damage to equipment.[7] Amine functionalized solid sorbents have been explored as potential alternatives for CO_2 capture.[8] These are porous materials surface-modified with organic amine functionality capable of high selectivity and high CO_2 sorption capacities at low CO_2 partial pressure.[9]

The polyamine polyethyleneimine (PEI, Figure 1) has been studied widely for the purpose of CO_2 sorption.[9-10] It has a high amine loading at one amine per two carbon atoms, with the branched form of PEI containing primary, secondary, and tertiary amines in a roughly 1:1.2:0.76 ratio according to the manufacturer.[11] Generally, solid PEI-based CO_2 sorbents feature amines impregnated or covalently tethered to silica support materials,[12-15] resins, including polymethacrylate,[16] and zeolites.[17] Although highly promising, impregnated materials face challenges such as amine leaching.[18-19] Furthermore and fundamentally, the support materials reduce the potential CO_2 sorption capacity by the addition of weight, which nevertheless still takes in energy during regeneration of the sorbent; an energy intensive process which continues to pose a particular challenge in CO_2 capture technologies.[5]

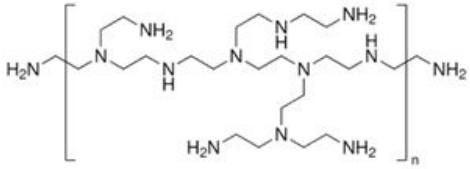

PEI

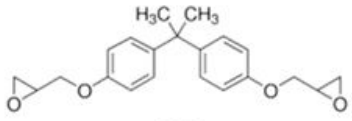

DER

Figure 1. Chemical structures of PEI and DER.

One alternative to using a support is to employ cross-linking, anchoring points along the polyamine chains, thereby creating an extended network of maximum amine content capable of high sorption. This technique is seldom reported in the literature, however it has started to show promising results. Our research is focused on understanding how cross-linking can enhance polyamine performance toward carbon capture.[20-25] In particular, we have previously identified a highly selective and effective sorbent material in the form of PEI 25,000 Da cross-linked by C_{60}.[25] It was observed that the CO_2 uptake at equilibrium of PEI-C_{60} outperformed that of the metal-organic framework Mg-MOF-74, at low pressure and high temperature, typical of power and industrial flue gas emissions. At conditions of 1 bar, 90 °C, sorption reached 0.20 g/g (4.55 mmol CO_2/g), and at 0.1 bar it was double the adsorption of Mg-MOF-74. PEI-C_{60} also showed very high selectivity over CH_4 and N_2, a vital criterion for efficient capture of CO_2 from flue gas systems.

This material expanded our class of support-free CO_2 sorbents in that the bulk of the material is the CO_2 sorbent-active component PEI, with the cross-linker simply serving to form a solid without constituting a majority of the resulting material mass. In a similar approach to ours, Hwang et al. cross-linked PEI with glutaraldehyde, forming spherical particles of 0.1 – 0.2 μm in diameter, with a CO_2 sorption capacity increasing with the degree of cross-linking, up to 2.18 mmol CO_2/g at 90 °C.[26]

Herein, we further explore cross-linking as a means of synthesizing sorbents, and in an effort to find a suitable cross-linking replacement for the nanomaterial, we use the vastly more economical cross-linker epoxy resin bisphenol-A diglycidyl ether (D.E.R.™ 332, DER in short, Figure 1).

Epoxy resins are pre-polymer compounds featuring more than one epoxy group per molecule.[27] They are extremely versatile and widely used materials, having an extensive variety of applications including paints, varnishes, floorings, reinforced composites,[28] adhesives,[29] and the encapsulation of semiconductor devices.[30-31] While their final properties are dependent on the method of their polymerization,[32] their advantages over other resins and thermosetting plastics include their high mechanical strength, chemical resistance, adhesion properties and electric resistivity, and low shrinkage or release of volatile by-products during the curing process.[33] They have also been used in combination with other polymers to form interpenetrating polymer networks of high strength and stiffness.[34] One of the most commercially significant epoxy resins are the glycidyl ethers. For use in their broad number of technological applications, epoxy resins are polymerized via the epoxy rings to form a robust, covalently-bonded three-dimensional network. A polyfunctional curing agent, or hardener, polymerizes the epoxy in a cross-linking reaction as a co-monomer; these include acid anhydrides and compounds possessing active hydrogen atoms including primary and secondary amines, phenols, alcohols, thiols and carboxylic acids. Generally, high cross-linking densities are required for epoxy resins to achieve their highest physical performance for their typical uses, therefore for curing purposes, reactants are used in near stoichiometric quantities.[35]

For several decades, amines, specifically aliphatic and aromatic amines, have been among the most commonly employed curing agents for epoxy resins.[36 37] The basic reaction scheme for the amine-epoxide reactions for primary and secondary amines, resulting in secondary and tertiary amines respectively, is shown in Figure 2(a) and (b).

PEI based polymers have been identified as useful curing agents for epoxy resins to impart qualities such as flame retardance.[38] They have also been used in conjunction with epoxy resins for the gel casting of ceramics,[39] and in the uniform coating of epoxy composites with carbon nanotubes.[40]

Supported CO_2 sorption materials have been synthesized using epoxy resin to cross-link PEI. Li et al. coated a glass fiber matrix with PEI cross-linked with epoxy resin,[41] and Jung et al. cross-linked PEI with 1,3-butadiene diepoxide, before impregnating onto silica. The resulting sorbent showed increased thermal stability and resistance to physical degradation by leaching and evaporation.[42] In both instances the cross-linker served to improve the performance of the material by increasing the thermal stability.

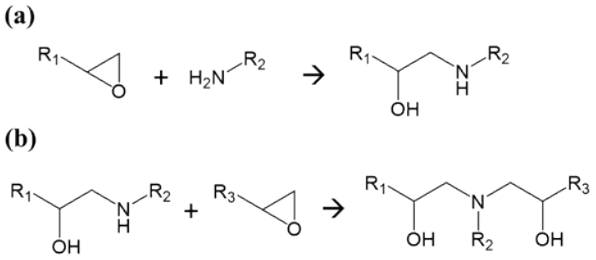

Figure 2. (a) Amine-epoxy reaction with primary amine, (b) secondary amine.[43]

Water stability presents a major challenge to CO_2 capture materials. Moisture is often detrimental to CO_2 uptake by solid sorbents that take up CO_2 primarily through physisorption such as MOFs and zeolites due to low stability to water vapor and competition for the active adsorption sites. Therefore, hydrophobic functionality is commonly employed to improve the performance of such sorbents.[44-45] Solid amine CO_2 sorbents have a natural advantage over such materials however, in that the presence of water can be beneficial by leading to the formation of ammonium bicarbonate. This sorption pathway would theoretically enable each amine to take up one CO_2 molecule, as opposed to the two amines required to absorb one CO_2 molecule under dry conditions.[46-47] However, diffusion limitations pose major challenges to the sorption capability of solid amine supports due to dense packing of the amines within pores.[48-49] In this case, hydrophobicity can again be usefully employed to improve sorption performance. To overcome the problem of diffusion and increase CO_2 sorption on PEI-impregnated MCM-41, Heydari-Gorji and Sayari improved the dispersion of PEI by introducing a surface layer of hydrophobic cetyltrimethylammonium surfactant cations onto the silica support.[50] With CO_2.sorption of 0.206 g/g at 75 °C, the material with 55% PEI loading was a more superior sorbent to comparable materials. This sorption performance was put down to reduced diffusion resistance of CO_2 within the material which was associated with greater dispersion of PEI on the hydrophobic surface layer.

For power and industrial applications such as flue gas CO_2 capture, where the partial pressure of CO_2 is low, increasing the interaction between amine groups and CO_2 is fundamental to

maximizing sorption and hydrophobicity can play a valuable role in the design of suitable materials. In our previous research on PEI-C_{60}, we proposed that the high sorption observed was due to the hydrophobic nature of the fullerene, bringing about non-affinity repulsive interactions between C_{60} and the hydrophilic amines, which forces the externalization of amine groups, activating the material towards CO_2 sorption.[25]

Further investigating the concept that the activation of PEI to CO_2 sorption is a function of the hydrophobic C_{60} cross-linker, we carried out work on C_{60} cross-linked polypropylenimine (PPI).[21] It was calculated that the overall energy barrier of CO_2 sorption decreased with increasing C_{60} content, likely due to the disruption of the hydrogen bonding network between the amino groups and sorbed water. However, the presence of C_{60} also lowered the probability of reaction due to the greater mobility of the amines, therefore lowering the probability of achieving reorganization of the amine and CO_2 for successful collision (sorption).

In this work, we synthesize self-supported DER cross-linked PEI materials suitable for CO_2 capture, following our approach of cross-linking to eliminate the need for a support and progressively decreasing the non-sorbent component to a minimum, aiming towards a more efficient sorbent. Furthermore, a proof-of-concept is demonstrated whereby the cross-linked PEI material sorption behavior is improved by hydrophobic functionalization of the polyamine chain. Prior to cross-linking with DER, PEI is reacted with various epoxy additives shown in Figure 3. These functionalized materials display enhanced CO_2 sorption behavior at 90 °C, and are shown to reach their optimum sorption at lower temperatures compared to the unfunctionalized PEI:DER material. One branched chain hydrocarbon additive-modified material exhibits CO_2 sorption of 0.101 g/g at 0.1 bar, and 0.195 g/g at 1 atm CO_2. This material also has high CO_2 selectivity and a good working capacity under sorption cycles in a 10% CO_2/90% N_2 mixture. It is also demonstrated that humidity can improve its sorption behavior at lower temperature.

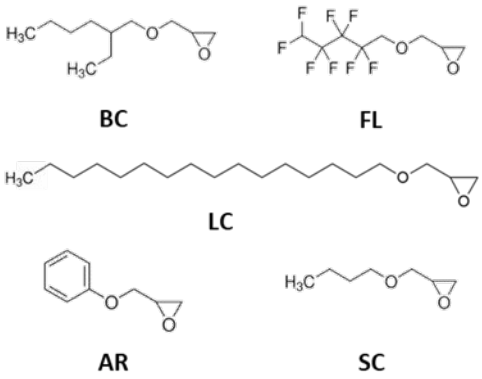

Figure 3. Chemical structures of additives. 2-Ethylhexyl glycidyl ether (BC), glycidyl 2,2,3,3,4,4,5,5-octafluoropentyl ether (FC), glycidyl hexadecyl ether (LC), 1,2-epoxy-3-phenoxypropane (AR) and butyl glycidyl ether (SC).

EXPERIMENTAL SECTION

Chemicals. All chemicals and solvents were purchased from Sigma-Aldrich, except from deuterated chloroform, which was purchased from Goss scientific, Chloroform-D (99.8%). All chemicals were used without further purification. Chloroform (≥99.8%), petroleum ether (≥90%), branched polyethyleneimine (PEI, Mw = 25,000 Da), D.E.R.™ 332 (DER, 340.41 g/mol), glycidyl 2,2,3,3,4,4,5,5-octafluoropentyl ether (FL, 288.14 g/mol, 96%), 2-ethylhexyl glycidyl ether (BC, 186.29 g/mol, 98%), glycidyl hexadecyl ether (LC, 298.50 g/mol, technical grade), 1,2-epoxy-3-phenoxypropane (AR, 150.17 g/mol, 99%), butyl glycidyl ether (SC, 130.18 g/mol, 95%). Pureshield Ar (99.998%) and CO_2 (99.8%) gases were supplied by BOC, and 10.14% CO_2/N_2 (±2%) was supplied by Air Liquide.

Materials Synthesis. PEI:DER samples were prepared by adding a 0.580 mol L^{-1} chloroform solution of DER (525 µL, 0.305 mmol; 262 µL, 0.152 mmol; or 169 µL, 0.098 mmol) along with 474 µL, 734 µL or 824 µL of chloroform respectively, to a 2 g aliquot of PEI dissolved in chloroform (25% w/w). The reaction mixtures were stirred and heated at 50 °C overnight then the resulting gels were crushed with a mortar and pestle and washed in approx. 10 mL of petroleum ether and stirred at 50 °C for approx. 1 hour. On removing the petroleum ether, the samples were placed in a vacuum oven for 3 nights then stored in a desiccator. Once dried, the products appeared as solid, white to pale yellow plasticky materials. The functionalized PEI:DER materials were prepared by adding BC (134 µL, 0.719 mmol; 56 µL, 0.268 mmol; or 36 µL, 0.172 mmol), LC (173 mg, 0.580 mmol; 87 mg, 0.291 mmol; or 58 mg, 0.194 mmol), FC (110 µL, 0.576 mmol; 56 µL, 0.295 mmol; or 37 µL, 0.194 mmol), AR (85 µL, 0.566 mmol; 43 µL, 0.320 mmol; or 31 µL, 0.226 mmol), or SC (86 µL, 0.599 mmol; 40 µL, 0.277 mmol; or 25 µL, 0.177 mmol) additive to a 2 g aliquot of PEI dissolved in chloroform (25% w/w). The reaction mixtures were stirred and heated at 50 °C overnight. Subsequently, a 0.580 mol L^{-1} chloroform solution of DER (262 µL, 0.152 mmol) and 737 µL of chloroform were added and the cross-linked products were prepared as before.

Materials Characterization. CHN data were collected on an Elementar vario MICRO cube. Approx. 2 mg of sample was weighed into tin boats for analysis. A ceramic ash crucible was placed into the combustion tube for the analysis of fluorinated samples. ^{1}H NMR measurements were performed at room temperature unless otherwise stated on a Bruker Avance III 500 MHz spectrometer, and all chemical shifts are reported in ppm. ^{1}H NMR spectra were referenced to the residual protio isotopomer present in $CDCl_3$ (7.26 ppm). A Thermo Scientific Nicolet iS10 FT-IR Spectrometer was used to collect the attenuated total reflectance infrared spectra of all samples. Spectra were recorded in the 650 – 4000 cm^{-1} region with 16 scans.

CO_2 Sorption Analysis. CO_2 Uptakes: All gravimetric gas uptake measurements were recorded using a TA Instruments SDT Q600 thermogravimetric analysis/differential scanning calorimeter (TGA/DSC) and the sample was placed in an open alumina crucible. Prior to purging the sample, argon (Ar) was filtered through a Perkin Elmer Ultra Clean Moisture Filter. Isothermal CO_2 capture tests were carried out at 1 atm in the following sequence: (i) activation to remove the preabsorbed species at 110 °C under Ar flow for 6 hours; (ii) reduction of the temperature to 90 °C or maintain at 110 °C, followed by initiation of gas uptake by flowing dry CO_2 at atmospheric pressure for 10 hours. Each step was performed until

equilibration. Temperature ramp CO_2 capture tests were carried out at atmospheric pressure in the following sequence: (i) activation to remove the preabsorbed species at 90 °C under Ar flow; (ii) reduction of the temperature to 40 °C followed by initiation of gas uptake by flowing dry CO_2 at atmospheric pressure. The temperature was increased at a rate of 0.1 °C/min until 150 °C; (iii) isothermal for 30 minutes then the temperature was reduced at 0.1 °C/min until 40 °C; isothermal for 60 minutes. Cyclic sorption/desorption CO_2 uptake experiments were carried out at atmospheric pressure in the following sequence: (i) activation to remove the preabsorbed species at 120 °C under Ar flow for 1 hours 30 minutes; (ii) reduction of the temperature to 90 °C, followed by initiation of gas uptake by flowing dry 10% CO_2/N_2 at 1 atm for 15 minutes; (iii) increase of the temperature to 155 °C, followed by initiation of gas desorption by flowing dry CO_2 at 1 atm for 5 minutes. Then step (ii) and (iii) were repeated for each cycle. For these experiments the gas used during desorption was set with a flow rate of 100 mL/min, and the gas for sorption with a flow rate of 95 mL/min. Pre-hydration experiments: Water uptake and CO_2 sorption experiments were carried out at atmospheric pressure in the following sequence: (i) activation to remove the preabsorbed species at 155 °C under Ar flow for 1 hour 30 minutes; (ii) the temperature was then reduced and stabilized at 25 °C (iii) the sorbent was then equilibrated to a constant weight under a 80 mL/min stream of Ar humidified using a water-filled bubbler; (iv) the gas was then switched to a humid stream of CO_2 with a flow rate of 80 mL/min, (calculated as 21.4% RH)[20] for 4 hours; (v) the material was subsequently desorbed under a flow of dry Ar at 100 mL/min for 8 hours; (vi) desorption was continued once the temperature was ramped to 155 °C for 1 hour 30 minutes.

Gas sorption isotherms: A Quantachrome iSorb HP1 High Pressure Gas Sorption Analyzer was used to collect sorption data. Cell void volume was calibrated by introducing helium in two stages: first at 45 °C, then at the analysis temperature using an external temperature controlling system. Prior to CO_2 sorption studies, the material was degassed under vacuum at 110 °C for 3 hours using a heating ramp rate of 10 °C/min. Subsequent degassing prior to each isotherm collected was carried out at 90 °C for 90 – 120 minutes using a heating ramp rate of 10 °C/min. For each CO_2 isotherm, 12 – 15 data points were collected from 0.01 – 1 bar. For each data point, 5 equilibrium points were measured with a 30 second interval. The equilibrium threshold was set to 0.2 mbar/min. A 0.1531 g sample was used. Specific degassing and analysis conditions for each CO_2 isotherm are given in Table S1. Prior to the N_2 sorption study, the material was desorbed under vacuum at 120 °C for 240 minutes, using a heating ramp rate of 20 °C/min. For the N_2 isotherm at 90 °C, 10 data points were collected from 0.01 – 1 bar. For each data point, 5 equilibrium points were measured with a 30 second interval. The equilibrium threshold was set to 0.2 mbar/min. A 0.2578 g sample was used. During sorption, the temperature of the cell was maintained using an insulated thermal heat jacket. CO_2 isotherms were fitted using the Single Site Langmuir equation. The isosteric enthalpy of sorption (IES) data were calculated using the linear version of the Clausius-Clapeyron equation in the loading range 0.1-2.5 mmol/g.

RESULTS AND DISCUSSION

This work was focused on demonstrating the feasibility of synthesizing an economical and effective CO_2 sorbent from PEI without the requirement of a support material. Bisphenol-A diglycidyl ether, D.E.R.™ 332, or DER epoxy resin, was used to cross-link branched chain PEI 25,000 Da, in effect, using the polyamine as a 'hardener'. However, in contrast to the traditional curing of epoxy resins, the polyamine was used in vast stoichiometric excess to the epoxy resin so only a minority of the amines reacted, leaving the majority unreacted to maximize the number of amines available for CO_2 sorption. At the same time, the amount of epoxy resin had to be enough to modify the internal structure of the polymer sufficiently such that the normally viscous liquid PEI became a solid able to maintain its shape.

In order to establish the optimum cross-linking density, three PEI:DER materials were prepared with amine:epoxy molar ratios of 20:1, (PD20), 40:1 (PD40) and 60:1 (PD60). The starting materials, dissolved in chloroform, were reacted at 50 °C for 24 hours, forming a clear, colorless gel, indicative that the cross-linking reaction had occurred. PD40 formed a slightly softer gel than PD20 and was less sticky than PD60. The CO_2 sorption behavior of the samples was tested by TGA-CO_2 sorption studies carried out at both 90 and 110 °C (Figure S1). These temperatures were selected for sorption studies as they are relevant to post-combustion conditions, in which post combustion capture temperatures reportedly range in excess of 40 °C,[51-52] and up to around 150 °C.[53-54] All the materials performed better at 110 °C than at 90 °C. PD60 displayed the poorest sorption, with a maximum of 0.043 g/g at 110 °C. PD20 outperformed PD40 at 90 °C, with a maximum sorption of 0.106 g/g compared to 0.099 g/g, however at 110 °C, PD40 showed the best performance with a maximum sorption of 0.141 g/g compared to 0.128 g/g. Due to its higher overall performance, PD40 was selected for further sorption enhancement studies. Samples of PD40 were re-made, except the PEI was reacted with the additives prior to cross-linking with DER. PEI:additive (expressed in terms of amine:epoxy) molar ratios of 20:1, 40:1 and 60:1 were used. After cross-linking, the non-functionalized and functionalized samples were washed in petroleum ether and dried in a vacuum oven. The additive-functionalized PEI cross-linked samples were labeled after the abbreviations used for the additives (Figure 3), thus for the hydrocarbon branched chain (BC) additive the samples were named BC20, BC40, and BC60 for PEI:additive ratios of 20:1, 40:1 and 60:1, respectively. The same applies to all other additives as summarized in Table 1. SEM images of the PD40 and the 40:1 additive samples show a similar morphology (Figure S2–S7). Nitrogen sorption isotherms of these materials revealed that their surface area could not be measured using the Brunauer-Emmett-Teller (BET) method since no measurable nitrogen sorption could be detected by the instrument (Quantachrome Nova) at the temperature of analysis (77 K). The products of reaction were characterized using NMR, and the final products characterized with IR and CHN analysis. The sorption properties were investigated by TGA-CO_2 sorption experiments and the CO_2 selectivity of BC40 was tested by low pressure sorption analysis.

Table 1. Summary of sample abbreviations and corresponding amine:epoxy molar ratios.

Sample abbreviations	Amine (PEI) : epoxy (DER) molar ratio	Amine (PEI) : epoxy (additive) molar ratio
PD20; PD40; PD60	20:1; 40:1; 60:1	No additive
BC20; BC40; BC60	40:1	BC additive 20:1; 40:1; 60:1
LC20; LC40; LC60	40:1	LC additive 20:1; 40:1; 60:1
FL20; FL40; FL60	40:1	FL additive 20:1; 40:1; 60:1
AR20; AR40; AR60	40:1	AR additive 20:1; 40:1; 60:1
SC20; SC40; SC60	40:1	SC additive 20:1; 40:1; 60:1

Evidence of Formation of Functionalized Polyamine. The nucleophilic addition reaction of PEI and the additives, and that of PEI and DER, were investigated by ^{1}H NMR. To study the reaction between PEI and the additives, each were reacted with PEI overnight and the ^{1}H NMR spectra were obtained on the products formed. The region of interest, where peaks related to the opening of the additive epoxy group can be observed in the spectra, is between δ 2.8 and δ 4.0 ppm (Figure S8).

The NMR data of the functionalized PEI products before cross-linking are shown in Figure 4. The NMR spectra of the products generally show broad signals of unassignable multiplicity due to reaction with the polymer and shifted upfield relative to the spectra of the additives alone, due to the different chemical environment. For FL40, BC40 and SC40, the alkyl H atoms either side of the ether group (H1' and H2') can be assigned. The data suggest complete reaction of the additives with PEI due to the significant differences in the NMR spectra of the starting materials and the spectra of the products, including the number of peaks (see Figures S9 – S13). More specifically, the signal of the hydrogen adjacent to the epoxy group is not present in the products' spectra, and rather, there is the evolution of a new signal from the hydrogen next to the secondary hydroxyl group, (H3') formed from ring-opening. In AR40, this signal appears at δ 3.73 ppm, followed by a peak at δ 3.61 ppm indicative of the alkyl CH_2 hydrogens. For all the other functionalized PEI products this peak appears within a broad multiplet, featuring two signals. The most downfield appears at δ 3.48 ppm for SC40, δ 3.49 ppm for BC40, δ 3.54 ppm for LC40 and δ 3.61 ppm for FL40. This signal can be attributed to H3'. The second, less intense signal appears approx. δ 0.07 ppm further upfield. This signal may originate from the presence of a minor product, whereby the amine attacked the more substituted carbon of the epoxy group. It is likely the signal of the hydrogen atoms next to the primary hydroxyl group (Figure S14). That AR40 does not have evidence of the formation of a minor product suggests that the steric bulk of the aromatic ring directed reaction at only the less substituted carbon.

Evidence of Formation of Cross-linked Species. The gelation reaction between PEI and DER during cross-linking was investigated by in-situ NMR experiments. Experiments were

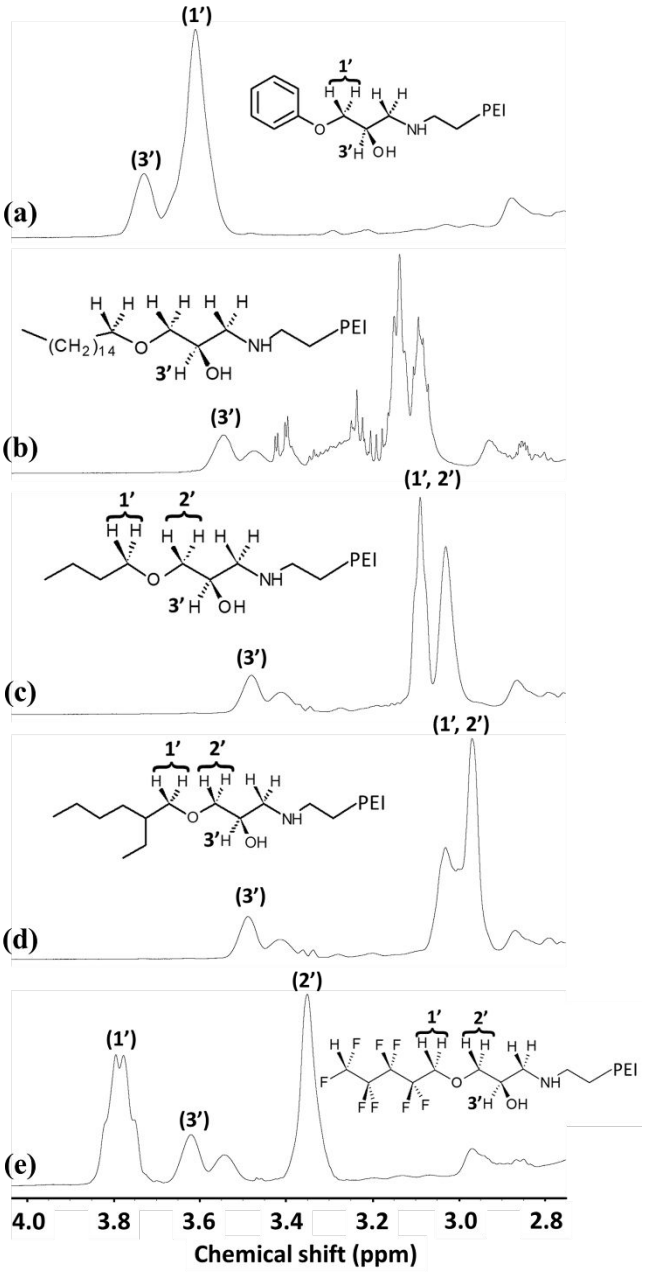

Figure 4. Expansion of the 500 MHz ^{1}H NMR spectrum of functionalized PEI before cross-linking, in $CDCl_3$, from δ 2.8 to δ 4.0 ppm. (a) AR40 spectrum showing a multiplet at δ 3.73 and 3.61 ppm corresponding to H3' and H1', respectively. (b) LC40 spectrum showing a multiplet at δ 3.54 ppm corresponding to H3', and a multiplet at δ 3.48 ppm corresponding to a minor product. Multiplets thereafter are unassignable. (c) SC40 spectrum showing multiplets at δ 3.48 and 3.06 ppm corresponding to H3', and H1' and H2', respectively. The multiplet at δ 3.41 ppm corresponding to a minor product. (d) BC40 spectrum showing multiplets at δ 3.49 and 3.00 ppm corresponding to H3', and H1' and H2', respectively. The multiplet at δ 3.41 ppm corresponding to a minor product. (e) FL40 spectrum showing multiplets at δ 3.78, 3.61, and 3.35 ppm corresponding to H1', H3', and H2', respectively. The multiplet at δ 3.54 ppm corresponding to a minor product.

run on samples with a 10:1 and 50:1 amine:epoxy molar ratio at 50 °C. However, while the 10:1 PEI:DER sample formed a gel, the 50:1 sample remained liquid, possibly due to the different heat distribution of the samples in the NMR experiment and those under standard laboratory conditions. From the spectra shown in Figure 5 it is apparent that DER is not fully consumed as the final spectra obtained during reaction features peaks related to DER, shifted upfield. However, the signal between δ 3.68 and δ 3.98 ppm features the emergence of a new peak (H3') at δ 3.88 ppm – which is unrelated to PEI – and can be assigned as that of the hydrogen next to the secondary hydroxyl group formed from ring-opening.

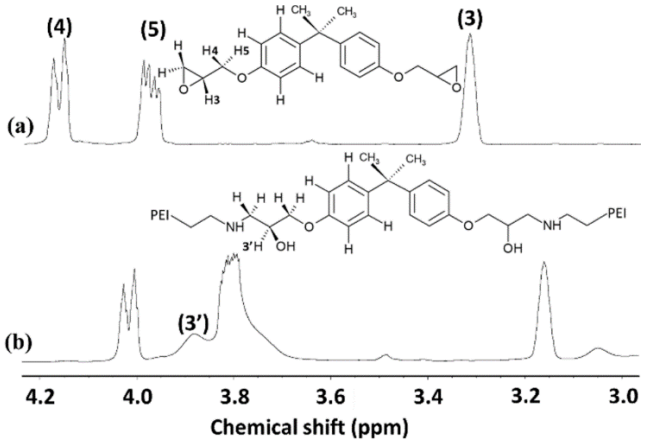

Figure 5. Expansion of the 500 MHz ^{1}H NMR spectrum of DER and PEI crosslinked with DER in a 10:1 amine:epoxy ratio in $CDCl_3$ at 50 °C, from δ 3.0 to δ 4.2 ppm. (a) DER spectrum showing two doublets of doublets at δ 4.17 and δ 3.98 ppm corresponding to H4 and H5, with the multiplet at δ 3.32 ppm corresponding to H3. (b) Spectrum of PEI crosslinked with DER, showing a multiplet at δ 3.88 ppm corresponding to H3'.

After cross-linking, the chemical skeletons of the final solid products were investigated by FTIR-ATR. Figure 6 shows the spectra of all the products along with the starting materials PEI and DER from 2000 – 600 cm^{-1}, and the full spectra of all the materials are compared, along with the additive starting materials in Figure S15.

In Figure 6, the products' spectra closely resemble that of PEI, with the polymer being the major component. All the epoxy starting materials display an absorption band between 903 and 915 cm^{-1} correlated to the asymmetric epoxy ring vibration, and they show various signals between 750 and 880 cm^{-1} which could correspond to the symmetric epoxy ring vibration. In the spectra of the product materials, the former band cannot be seen for the absorption of the PEI component, and there is a very small band at 827 cm^{-1}.[55] The absence or decrease of band intensity of the epoxy ring is expected due to the ring opening reaction during product formation, however it is apparent that there may remain residual unreacted epoxy groups.

The spectra of the functionalized samples all show a small band at around 1665 cm^{-1} relating to the H-O-H bending vibration of absorbed water, indicative of the hygroscopic character of the cross-linked polymer. The small sharp band at about 1508 cm^{-1} is due to C-C stretching vibrations of the aromatic rings of DER. There is a strong absorption peak at about 1455 cm^{-1} due to the CH_2 scissor vibration. The rather broad band at around 1294 cm^{-1} could be the CH_2 wagging vibration or the NH_2 rocking/twisting vibration. Residual epoxy may be evident in the band between 1245 and 1250 cm^{-1}, which may be related to the C-O stretching vibration, and the band at 1182 cm^{-1} may arise from the CH_2 twisting deformation vibration of the epoxy group.[55]

A secondary amine C-N stretching absorption band is observed near 1105 cm^{-1}. In FL40, there is a band at 1120 cm^{-1} which, along with the band at 1167 cm^{-1}, can be attributed to symmetric and asymmetric C-F_2 stretching vibrations respectively from the glycidyl 2,2,3,3,4,4,5,5-octafluoropentyl ether derivative. There is a primary amine C-N stretching absorption band at around 1037 cm^{-1} and a very broad band from the secondary amine N-H wagging vibration between 753 – 760 cm^{-1}. In the spectrum of AR40 however, the band at 753 cm^{-1} is far sharper.[55]

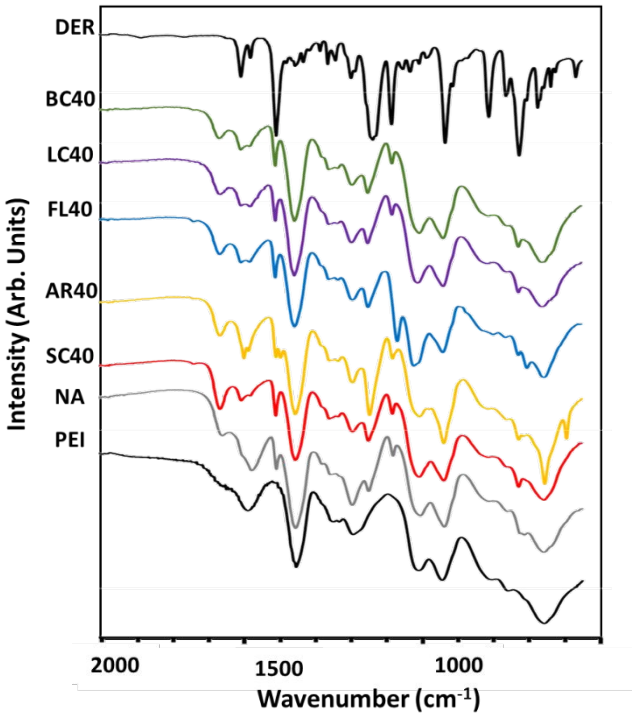

Figure 6. FTIR-ATR spectra of as-received PEI and DER against spectra of unfunctionalized (PD40, labelled as NA, no additive) and functionalized products.

Compositional Analysis. Elemental analysis was employed with a view to determining the stoichiometric ratio between PEI, DER and the additive, but due to the complexity of the materials, this information could not be obtained. However, the C/N ratio could be calculated, indicating as to whether the expected composition of the sample had resulted by comparing with the expected formula (PEI monomer)$_1$(DER)$_{(0.5/40)}$(additive)$_{(1/20;\ 1/40;\ 1/60)}$. The results are presented in Table S2, along with the % nitrogen content and the calculated amine efficiency of each sample during sorption.

As shown in Figure 7, for each set of samples, a pattern emerges whereby the sample with a PEI:additive (amine:epoxy) ratio of 20:1 has a lower C/N ratio than the calculated value, while the C/N ratios for the 40:1 and 60:1 samples are higher than their calculated values. This indicates that the 20:1 samples contain relatively more nitrogen and less carbon that intended, therefore they must feature less additive and/or less cross-linker, the latter being more likely given that these samples were synthesized with the highest ratio of additive (20:1) affecting the further reaction with the cross-linker. The 40:1 and 60:1 samples contain relatively more carbon than calculated. Generally, the 60:1 samples have a C/N ratio closer to that expected for the 40:1 samples (Table S2). In the case of BC, FL and SC, the C/N ratios for the 40:1 and 60:1 samples differ from each other by 0.04 or less (Table S2), while the 60:1 samples differ from their expected ratios by 0.13 or more. Because the 60:1 samples were synthesized with the least additive, the apparent higher relative carbon content than calculated likely originates from the cross-linker. This suggests that a lesser functionalized PEI polymer chain is more likely to react with an epoxy group of the DER and become bound into the solid product (there being more available amine groups and less steric hindrance). The result is a more densely cross-linked material. In the case of the 20:1 samples, the DER is less able to cross-link the more functionalized PEI chains resulting in a relatively less cross-linked product with higher relative nitrogen content than calculated.

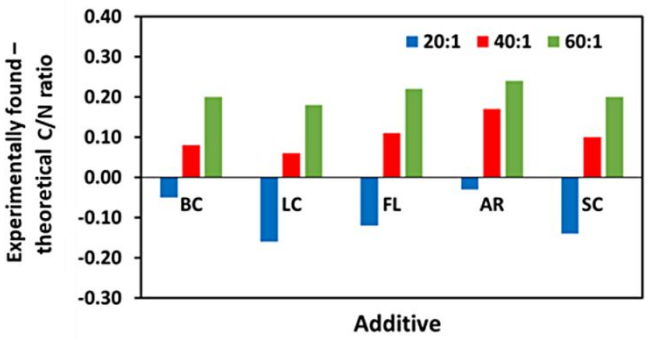

Figure 7. Difference between experimentally found and theoretical C/N ratio for all DER cross-linked samples with PEI:additive ratios 20:1, 40:1, and 60:1. For all samples the PEI:DER ratio is 40:1.

CO_2 Absorption Behavior. Our initial TGA-CO_2 sorption studies had shown that the PEI:DER materials take several hours to reach equilibrium and their maximum capacities (Figure S1), so, the CO_2 sorption studies of these materials were carried out over an extended period of 10 hours to allow their maximum capacity to be determined. The sorption behavior of PD40 against each group of functionalized samples were compared at 90 °C, as shown in Figure 8. 90 °C was selected as a temperature relevant to post-combustion CO_2 capture from flue gas. The corresponding maximum capacities are reported in Table S2 as the final measurement at 600 minutes. It is important to note that the samples show different kinetic behavior.

As shown in Figure 8(a – c), all functionalized samples show superior sorption performance to the unfunctionalized one, PD40, which shows a maximum sorption of 0.099 g/g (2.25 mmol/g). It is worth recalling that all the functionalized samples

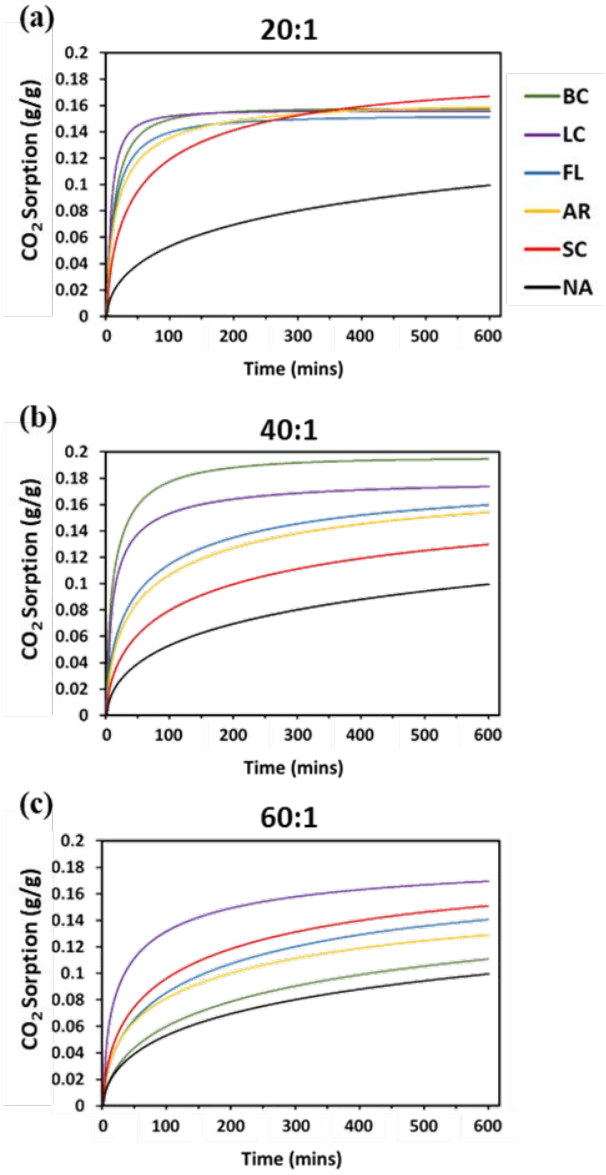

Figure 8. TGA-CO_2 sorption behavior g/g of (a) 20:1, (b) 40:1, and (c) 60:1 PEI:additive samples compared to PD40 (labelled as NA, no additive).

have PEI:DER ratios of 40:1, exactly like PD40. Figure 9 shows the amine efficiencies of all the samples under study, indicating that PD40 has the worst amine efficiency of 9.02 mol amine required to take up 1 mol CO_2. This demonstrates that any additive of any loading benefits sorption both in terms of capture capacity and amine efficiency.

The 20:1 samples generally show a narrow range of final sorption capacities from 0.151 g/g for FL20 to 0.167 g/g for SC20. The 40:1 samples however show a larger spread, from 0.130 g/g for SC40 to 0.195 g/g for BC40. BC40 is the highest performing sorbent, and indeed is the highest performing of all the reported samples, with a final CO_2 sorption of 0.195 g/g (4.43 mmol/g) at 90 °C in 1 atm CO_2. BC40 also has the highest amine efficiency of all the reported samples at 4.11 mol amine/mol CO_2. The 60:1 samples show a narrower spread of

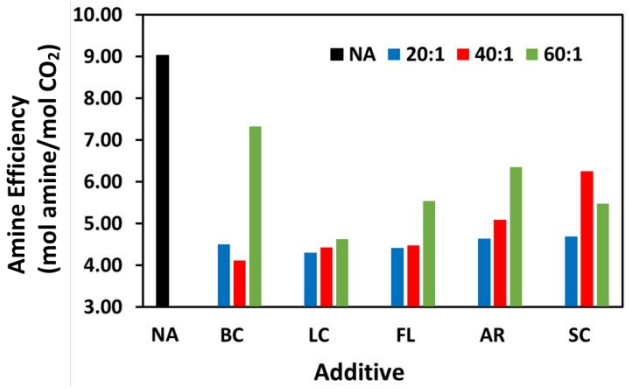

Figure 9. Amine efficiency of PEI:DER cross-linked sample with no additive (NA, corresponding to sample PD40) and all additives as PEI:additive ratios 20:1, 40:1, and 60:1. Amine efficiencies were calculated considering all amines, including tertiary amines of branched PEI.

final sorption capacities, and for each additive, the 60:1 samples show lower sorption compared to the 40:1 samples, except for SC. However, LC60 still shows high sorption at 0.169 g/g. These results suggest that with sufficient loading of any additive, a high sorption can be achieved, with an average of 0.158 g/g for the 20:1 samples. However, with less loading, the type of additive becomes more significant, and higher sorption is theoretically possible due to more free amines. That BC, LC and FL show the highest sorptions of the 40:1 samples, suggests that the longer bulkier samples most benefit sorption, but this is not fully reflected in the 60:1 samples where it is LC, SC and FL that show highest sorption and with BC60 showing the lowest sorption.

The BC and LC samples are similar in that it is the 40:1 sample which shows the highest CO_2 sorption, with LC40 reaching 0.174 g/g, however, it is LC20 which shows the best amine efficiency of the LC group at 4.30 mol amine/mol CO_2. Similarly, for the FL samples it is FL40 which shows highest CO_2 sorption at 0.160 g/g, but FL20 with the best amine efficiency at 4.41 mol amine/mol CO_2. The AR and SC samples show the highest CO_2 sorption for AR20 and SC20, at 0.159 g/g and 0.167 g/g respectively, and it is these samples which also have the highest amine efficiencies in their groups at 4.46 and 4.69 mol amine/mol CO_2 respectively. Except for the BC and SC group, the amine efficiency for all additives improves sequentially from 60:1 to 40:1 to 20:1. Furthermore, the 20:1 samples generally show the fastest sorption behavior compared to the 40:1 and 60:1 samples. Given that the 20:1 samples are less cross-linked than intended may explain why they generally show the highest amine efficiencies: the CO_2 molecules may be more able to diffuse into the less densely cross-linked polymer network and react with the available amines. It appears therefore, that the more functionalized and less cross-linked materials have higher amine efficiencies, if not consistently the highest absolute CO_2 sorption.

To contrast the sorbents and explore how their sorption behaviors change with temperature, the 40:1 sample from each group was selected and subjected to a temperature ramp from 40 °C to 150 °C and back down to 40 °C at a ramp rate of 0.1 °C/min, under a constant flow of CO_2, 1 atm, as shown in Figure 10. On increasing temperature (1st event), all the samples show increasing sorption until they reach a specific 'optimum sorption temperature' (OST). Thereafter, increasing temperature until 150 °C results in desorption, at which temperature all the samples, except for PD40, reach a weight minimum less than the initial weight of the fully desorbed material, suggesting further desorption at 150 °C, since samples were conditioned at 90 °C. However, on decreasing the temperature to 40 °C (2nd event), the samples re-sorb until equilibrium is reached. For the first sorption event from 40 to 150 °C, the samples OSTs, their corresponding CO_2 sorption capacities and amine efficiencies are shown in Table 2 and presented in Figure 11. The corresponding TGA-CO_2 sorption behavior of the samples is shown in Figure S16.

The functionalized samples all have lower OSTs, and except for SC40, reach higher sorption capacities and have better amine efficiencies than PD40. BC40 and LC40 have the lowest OSTs at 95.1 °C and 96.4 °C, at which temperatures their sorption capacities are the highest at 0.164 g/g and 0.154 g/g,

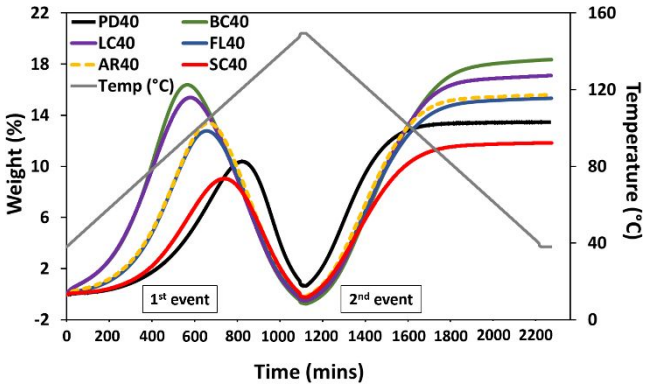

Figure 10. TGA-CO_2 sorption behavior (weight %) of all PEI DER-cross-linked samples during temperature ramps from 40 °C to 150 °C and back at 0.1 °C/min under constant flow of CO_2. Two sorption events are identified: one during heating (1st event) and the other one during cooling (2nd event).

Table 2. OSTs, CO_2 sorption capacities and amine efficiencies for the 40:1 functionalized materials and PD40 during the first sorption event (Figure 10).

CO_2 Capture Performance Upon Heating (1st event)			
Sample	OST (°C)	CO_2 peak sorption (g/g)	Amine Efficiency (mol amine/mol CO_2)
BC40	95.1	0.164	4.88
LC40	96.4	0.154	5.00
FL40	104.1	0.128	5.93
AR40	105.0	0.134	5.85
SC40	112.5	0.090	8.93
PD40	120.6	0.104	8.60

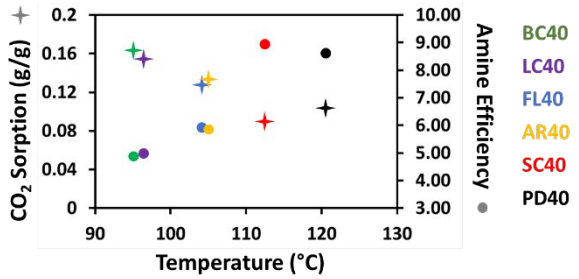

Figure 11. CO_2 peak sorption (✦) and amine efficiencies (●, mol amine/mol CO_2) against OST for the 40:1 functionalized materials and PD40.

respectively. These samples also have the best amine efficiencies at 4.88 and 5.00, respectively (mol amine/mol CO_2). Thereafter, the OSTs continue to increase in the order of FL40, AR40, SC40, PD40, with the sorption capacities decreasing from 0.134 g/g for AR40, to 0.091 g/g for SC40 and the amine efficiencies ranging from 5.85 to 8.93 (mol amine/mol CO_2) for AR40 and SC40 respectively. The OSTs for the functionalized samples may be lower due to the hydrophobic functionality of the additives creating repulsive interactions forcing greater exposure of the amine groups to CO_2,[21] therefore less energy is required for CO_2 diffusion and subsequent sorption. The results suggest that BC and LC, the longest and bulkiest of the additives, are the most effective for introducing hydrophobic functionality, followed by FL and AR, with SC, the shortest and smallest additive having the least impact on sorption capacity and amine efficiency when compared to PD40, although it does clearly lower the OST.

The results for the second sorption event from 150 – 40 °C (Figure 10) are shown in Table 3, and the corresponding TGA-CO_2 sorption behavior (g/g) of the samples is shown in Figure S17. The samples all immediately begin to re-sorb CO_2 upon cooling and once the OST is reached, they continue sorbing until reaching a plateau capacity at 40 °C. Their maximum sorption capacities are higher than reported for the first sorption event, likely due to the temperature reaching the samples OST, then reducing to below this temperature, which does not promote desorption of pre-sorbed CO_2. The capacities are in the same order as before, with BC40 reaching 0.192 g/g, and SC40 being the lowest reaching 0.121 g/g with PD40 slightly higher at 0.126 g/g.

In the second sorption event, it is interesting to compare the sorption capacities at the OSTs with the peak sorption capacities of the first event. LC40, BC40 and FL40 reach 0.149 g/g, 0.157 g/g and 0.122 g/g respectively, which are 96.8%, 95.7% and 95.3% respectively of their peak sorption capacities from the first event. AR40 and SC40 reach 0.124 g/g and 0.085 g/g, which are 92.5% and 94.4% respectively of their peak sorption capacities of the first event. PD40 on the other hand, reaches 0.089 g/g, which is 85.6% of its peak sorption capacity from the first sorption. This observation would seem to suggest that the functionalized samples are able to re-sorb faster than the unfunctionalized sample on reaching their OST for the second time and are therefore more robust to sorption/desorption cycles. Sorption/desorption cyclability is further address later in the paper.

The sorption data shows that the functionalization of PEI by the additives improves sorption performance relative to the unfunctionalized cross-linked material and reduces the optimum sorption temperature. The ability to potentially tune this temperature is highly significant in the development of CO_2 sorbents for different purposes, for example capture from flue gases, or in the development of materials designed to capture directly from ambient air.

The increase in sorption is most likely due to hydrophobic interactions introduced by the additives in that the presence of the hydrocarbon and fluorocarbon functionalities disrupt the hydrogen bond network between the amines and between sorbed water. The top performing materials overall are BC40 and LC40, suggesting that the longer and branched hydrocarbon additives are the most beneficial to sorption, however there is significant variability in sorption performance depending on the amount of additive introduced. While the 40:1 sample is also the best sorbent in the FL group, in the AR and SC groups, 20:1 is the best performing sample. This indicates that there must be a fine balance between the size, shape and bulk of an additive with the amount of additive loaded, with the smaller additives generally requiring higher loadings to introduce sufficient hydrophobic functionality to maximize CO_2 sorption.

Table 3. Maximum CO_2 sorption capacity of the 40:1 functionalized materials and PD40 upon cooling to the final temperature of 40 °C (Figure 10). The capture capacity during the second sorption event at the OST observed during the first sorption event, and this value as a percentage of the CO_2 peak sorption recorded in the first event.

CO_2 Capture Performance Upon Cooling (2nd event)			
Sample	Final (plateau) CO_2 abs at 40 °C (g/g)	CO_2 sorption at OST of each sample (g/g)	CO_2 sorption at OST as % of first maximum sorption
BC40	0.192	0.157	95.7 %
LC40	0.175	0.149	96.8 %
FL40	0.156	0.122	95.3 %
AR40	0.157	0.124	92.5 %
SC40	0.121	0.085	94.4 %
PD40	0.126	0.089	85.6 %

As the best performing material, the sorption behavior of BC40 was selected for further investigation to establish its potential for development as an industrial post-combustion CO_2 sorbent. In order to compare the sorption selectivity of CO_2 over N_2, sorption isotherms were collected over the range 0.01 – 1 bar at 90 °C for both gases. As shown in Figure 12, sorption of CO_2 is slightly lower than its expected capacity at 0.172 (g/g) at 1 bar, however, the sorption of N_2 is negligible up to 1 bar. The Ideal Adsorbed Solution Theory (IAST)[56] model was applied to infer the selectivity of BC40 for CO_2 under flue gas conditions. The partial pressures of CO_2 and N_2 were taken to be 0.10 bar and 0.90 bar respectively, (representative of the partial pressure of CO_2 from a natural gas-fired power plant). At these pressures, BC40 takes up about 0.10072 g/g CO_2 and 0.00034 g/g N_2, (Figure S18). These values give BC40 a selectivity factor of 2666 in favor of CO_2 capture.

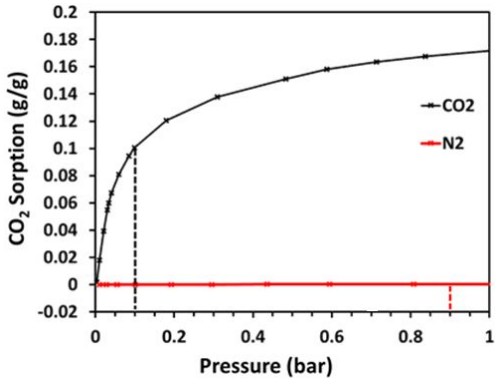

Figure 12 Selectivity of CO_2 uptake of BC40. Single component CO_2 and N_2 sorption (g/g) at 90 °C in the low-pressure range. The dashed lines indicate the corresponding interpolated uptakes at the representative pressures of flue gas: 0.10 bar CO_2 and 0.90 bar N_2.

Further sorption isotherms for CO_2 were measured at 80, 100 and 110 °C (Figure S19) and compared to that at 90 °C. These show that, on decreasing temperature, the CO_2 uptake curve becomes steeper and the sorbent reaches saturation at lower pressure. It can be seen from the kinetic data for these isotherms (Figure S20) that, except for the first gas dose at 0.01 bar, the system systematically reaches equilibrium much more slowly at lower temperature, indicating significant diffusion limitations that can be overcome by increasing the temperature.

The isosteric enthalpy of sorption (IES) provides a measure of the strength of the interaction between the CO_2 and the sorbent. The IES was calculated from the CO_2 isotherms at 80, 90, 100 and 110 °C using the Clausius-Claperyon equation (Figures S21 -S24, and Table S3). The IES for CO_2 in BC40 declined from 63.1 kJ/mol at 0.1 mmol/g CO_2 loading, to 52.2 kJ/mol at 2.5 mmol/g loading (Figure S25). This confirms that the sorption mechanism is primarily chemical in nature and is much in line with other solid amine sorbents,[57] for which IESs range from 60 to 90 kJ mol^{-1}.[9]

To investigate the ability of BC40 to capture CO_2 from a gas mixture, the material was tested under conditions more representative of flue gas in a TGA-CO_2 sorption experiment using a 10% CO_2/90% N_2 mixture. The material's resilience to sorption/desorption cycles was also investigated by subjecting the sorbent to a repetitive CO_2 sorption/desorption program, mimicking a temperature swing process.[51] Sorption took place at 90 °C and 1 atm under a 10% CO_2 stream, whereas desorption took place at 155 °C and 1 atm under 100% CO_2, with each sorption/desorption cycle taking 33 minutes. As can be seen in Figure 13, the working capacity stays constant at 9.4 - 9.5 % over the course of 29 cycles, demonstrating good performance and excellent recyclability. This working capacity compares reasonably well to other sorbents such as the diamine appended MOF mmen-Mn_2(dobpdc), in which a working capacity of 10% was attained under a 15% CO_2/N_2 gas flow at 70 °C with desorption at 120 °C under pure CO_2.[51] There is some sample mass loss observed equating to about 1.3%. Sorbent mass loss has also been observed by Goeppert et al. in subjecting a supported amine-epoxide based CO_2 solid sorbent to similar sorption/desorption cycles at 85 °C. The authors suggest this was due to leaching of the amine, tetraethylenepentamine.[58] In our case, the same reasoning cannot be applied; the mass loss is likely due to residual strongly bound water being slowly removed while cycling, or it may have contribution from possible degradation of the material. Nevertheless, the working capacity remains stable. (Figure S26).

In order to evaluate the effect of moisture on the CO_2 uptake performance of BC40, the material was tested by a TGA-CO_2 sorption experiment with a series of steps under humidified conditions. The temperature for sorption analysis was 25 °C since water sorption is significant at lower, rather than higher, temperatures.[25] As shown in Figure 14, the pre-activated material was initially exposed to a flow of wet Ar, hydrating it to 0.672 g H_2O/g sorbent. It was then exposed to wet CO_2, and showing faster sorption kinetics than for water uptake, the overall

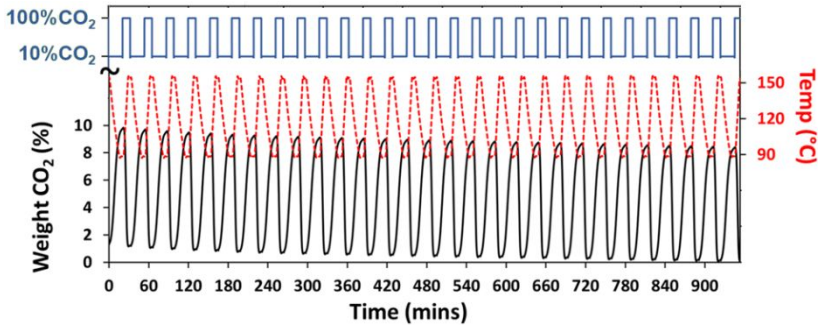

Figure 13. CO_2 sorption and desorption cycling isotherm for BC40 at 1 atm in which sorption occurs under a 10% CO_2/N_2 gas stream at 90 °C and desorption under pure CO_2 at 155 °C, utilizing a temperature swing process for regeneration. The working capacity is 9.4 - 9.5 % over the course of 29 cycles.

sorption mass reached 0.907 g/g. The difference 0.907-0.672 = 0.235 g/g corresponds to the amount of CO_2 captured in the water-saturated sorbent. The 0.235 g/g of CO_2 captured at 25 °C in wet conditions is 0.040 g/g higher than the 0.195 g/g sorbed in dry conditions at 90 °C (Figure 8(b)). The uptake of CO_2 in dry conditions at 25 °C is negligible (Figure S27), therefore it is clear that water promotes CO_2 sorption in BC40 at 25 °C. Furthermore, the kinetics of sorption is significantly increased in the presence of water (Figure S27). After reaching 0.907 g/g CO_2+H_2O sorption, the saturated material was exposed to dry Ar at 25 °C for desorption (Figure 14). As previously observed,[20] only part of the sorbed water is desorbed leaving in the materials 0.341 g/g of bound CO_2 and H_2O. The amount of bound H_2O can be estimated from 0.341-0.235 = 0.106 g/g, of which about 0.029 g/g is found to interact strongly with the sorbent material itself (Figure S28, showing water uptake alone followed by desorption at 25 °C under dry Ar leaving about 0.029 g/g of water bound to BC40). The corresponding CO_2:H_2O molar ratio is 0.91 mol/mol (0.235/44 mol to 0.106/18 mol), about one molecule of water per each molecule of carbon dioxide suggesting the possible formation of bicarbonate.

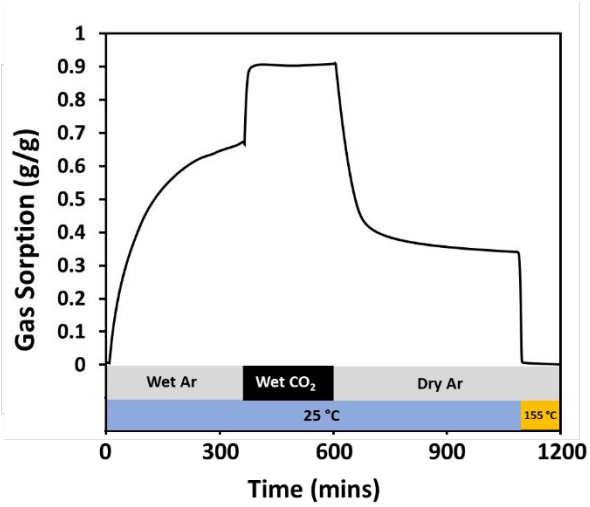

Figure 14. TGA of H_2O and CO_2 sorption behavior (gas sorption g/g) of BC40 under humidified conditions at 25 °C and 1 atm.

CONCLUSIONS

A new family of support-free CO_2 sorbent materials based on the DER cross-linking of PEI modified with selected additives is reported. The material without additive modification shows CO_2 sorption of 0.099 g/g, 2.25 mmol/g (1 atm, 90 °C). The addition of hydrocarbon or fluorocarbon additives, during synthesis, improves both sorption and amine efficiency, with the highest performing material, BC40 improving CO_2 uptake by 97% with sorption of 0.195 g/g (4.43 mmol/g). This material also shows high selectivity of CO_2 over N_2, good working capacity and excellent recyclability under sorption/desorption cycles (sorption: 10% CO_2/N_2, desorption: 100% CO_2), and improved uptake of CO_2 under humidified conditions at ambient temperature.

The sorption behavior of these materials appears to be dependent on both additive loading and the molecular structure of the additive. The additive loading likely affects the extent of the cross-linking reaction, with the 20:1 samples expectedly being the least cross-linked and 60:1 samples the most. Generally, the 20:1 samples have the highest amine efficiencies. It is possible that the lesser cross-linked functionalized materials are more permeable to CO_2, therefore allowing more amines to react with CO_2. The additives themselves introduce localized hydrophobic functionality, which repel and therefore expose the hydrophilic amines, making them more disposed to react with CO_2. This effect is generally seen to a greater extent for the larger, longer and bulkier additives, however for higher loadings the type of additive does not appear to have a large effect on the final sorption capacity. The additives appear not only to improve sorption, but also reduce the temperature at which the material displays its optimum sorption behavior as less heat is required to allow better diffusion of CO_2.

In wet gas streams, the kinetics of CO_2 sorption at lower temperatures (e.g. 25 °C) is drastically improved reaching > 0.2 g/g CO_2 in under 15 min. In terms of scalability, the kinetics of a larger sample size could be affected by the shaping and packing of the sorbent. These would have to be optimized in order to maintain sorbent accessibility resulting in improved CO_2 mass transport in the bulk of the material.

This work confirms the cross-linking approach as a valid and valuable means to make effective support-free CO_2 sorbents by utilizing an economical cross-linker. It also demonstrates the potential to improve and even tune the sorption behavior of these materials through the introduction of hydrophobic additives. The extent to which sorption can be increased, and the temperature of maximum sorption can be reduced, should now be explored by developing materials using additives of increasing chain length and complexity. In view of the overall aim to reduce non-sorbent mass as far as possible, while maintaining the structure and properties to enhance CO_2 sorption, the next step would be to combine the hydrophobicity of the additive with the structural functionality of the cross-linker and develop a material with an inexpensive hydrophobic cross-linker.

ASSOCIATED CONTENT

NMR data, FTIR data, TGA-CO_2 sorption profiles, N_2 sorption isotherms, CO_2 sorption isotherms and fitting parameters, isosteric enthalpy of sorption calculation, C/N ratios, CO_2 capacities and amine efficiencies, further material synthesis and characterization details supplied as Supporting Information. This material is available free of charge via the Internet at http://pubs.acs.org.

AUTHOR INFORMATION

Corresponding Author

***Email: e.andreoli@swansea.ac.uk**

ORCID

Louise B. Hamdy: 0000-0002-4929-9782

Russel J. Wakeham: 0000-0002-4304-0243

Marco Taddei: 0000-0003-2805-6375

Andrew R. Barron: 0000-0002-2018-8288

Enrico Andreoli: 0000-0002-1207-2314

Author Contributions

All authors have given approval to the final version of the manuscript.

Notes

The authors declare no competing financial interest.

ACKNOWLEDGMENT

This work is part of the Flexible Integrated Energy Systems (FLEXIS) and Reducing Industrial Carbon Emissions (RICE) research operations funded by the Welsh European Funding Office (WEFO) through the Welsh Government. Financial support was also provided by the Sêr Cymru Chair Programme, and the Robert A. Welch Foundation (C-0002).). We also acknowledge funding from the European Union's Horizon 2020 research and innovation program under the Marie Skłodowska-Curie grant agreement No 663830. The authors would like to acknowledge Dr Matthew J. McPherson for assistance in performing BET measurements.

ABBREVIATIONS

PEI, polyethyleneimine; BC, 2-ethylhexyl glycidyl ether; LC, glycidyl hexadecyl ether; FL, glycidyl 2,2,3,3,4,4,5,5-octafluoropentyl ether; AR, 1,2-epoxy-3-phenoxypropane; SC, butyl glycidyl ether; NA, no additive; OST, optimum sorption temperature; IAST, Ideal Adsorbed Solution Theory; IES, isosteric enthalpy of sorption.

REFERENCES

1. Friedlingstein, P.; Andrew, R. M.; Rogelj, J.; Peters, G. P.; Canadell, J. G.; Knutti, R.; Luderer, G.; Raupach, M. R.; Schaeffer, M.; van Vuuren, D. P.; Le Quéré, C., Persistent growth of CO2 emissions and implications for reaching climate targets. *Nature Geoscience* **2014,** *7*, 709.
2. Dell'Amico, D. B.; Calderazzo, F.; Labella, L.; Marchetti, F.; Pampaloni, G., Converting Carbon Dioxide into Carbamato Derivatives. *Chemical Reviews* **2003,** *103* (10), 3857-3898.
3. Bollini, P.; Didas, S. A.; Jones, C. W., Amine-oxide hybrid materials for acid gas separations. *Journal of Materials Chemistry* **2011,** *21* (39), 15100-15120.
4. Hahn, M. W.; Steib, M.; Jentys, A.; Lercher, J. A., Mechanism and Kinetics of CO2 Adsorption on Surface Bonded Amines. *The Journal of Physical Chemistry C* **2015,** *119* (8), 4126-4135.
5. Li, W.; Choi, S.; Drese, J. H.; Hornbostel, M.; Krishnan, G.; Eisenberger, P. M.; Jones, C. W., Steam-Stripping for Regeneration of Supported Amine-Based CO2 Adsorbents. *ChemSusChem* **2010,** *3* (8), 899-903.
6. Rochelle, G. T., Amine Scrubbing for CO₂ Capture. *Science* **2009,** *325* (5948), 1652-1654.
7. Martens, J. A.; Bogaerts, A.; De Kimpe, N.; Jacobs, P. A.; Marin, G. B.; Rabaey, K.; Saeys, M.; Verhelst, S., The Chemical Route to a Carbon Dioxide Neutral World. *ChemSusChem* **2017,** *10* (6), 1039-1055.
8. Ünveren, E. E.; Monkul, B. Ö.; Sarıoğlan, Ş.; Karademir, N.; Alper, E., Solid amine sorbents for CO2 capture by chemical adsorption: A review. *Petroleum* **2017,** *3* (1), 37-50.
9. Samanta, A.; Zhao, A.; Shimizu, G. K. H.; Sarkar, P.; Gupta, R., Post-Combustion CO2 Capture Using Solid Sorbents: A Review. *Industrial & Engineering Chemistry Research* **2012,** *51* (4), 1438-1463.
10. Yang, H.; Xu, Z.; Fan, M.; Gupta, R.; Slimane, R. B.; Bland, A. E.; Wright, I., Progress in carbon dioxide separation and capture: A review. *Journal of Environmental Sciences* **2008,** *20* (1), 14-27.
11. https://www.sigmaaldrich.com/catalog/product/aldrich/408727?lang=en&region=GB&gclid=EAIaIQobChMImM6lgKK54QIVw4ayCh1nRgnUEAAYASAAEgJqs_D_BwE (accessed 29/5/2019).
12. Zhang, W.; Liu, H.; Sun, C.; Drage, T. C.; Snape, C. E., Capturing CO2 from ambient air using a polyethyleneimine–silica adsorbent in fluidized beds. *Chemical Engineering Science* **2014,** *116* (Supplement C), 306-316.
13. Choi, W.; Min, K.; Kim, C.; Ko, Y. S.; Jeon, J. W.; Seo, H.; Park, Y.-K.; Choi, M., Epoxide-functionalization of polyethyleneimine for synthesis of stable carbon dioxide adsorbent in temperature swing adsorption. **2016,** *7*, 12640.
14. Li, K.; Jiang, J.; Tian, S.; Yan, F.; Chen, X., Polyethyleneimine-nano silica composites: a low-cost and promising adsorbent for CO2 capture. *Journal of Materials Chemistry A* **2015,** *3* (5), 2166-2175.
15. Sandhu, N. K.; Pudasainee, D.; Sarkar, P.; Gupta, R., Steam Regeneration of Polyethylenimine-Impregnated Silica Sorbent for Postcombustion CO2 Capture: A Multicyclic Study. *Industrial & Engineering Chemistry Research* **2016,** *55* (7), 2210-2220.
16. Chen, Z.; Deng, S.; Wei, H.; Wang, B.; Huang, J.; Yu, G., Polyethylenimine-Impregnated Resin for High CO2 Adsorption: An Efficient Adsorbent for CO2 Capture from Simulated Flue Gas and Ambient Air. *ACS Applied Materials & Interfaces* **2013,** *5* (15), 6937-6945.
17. Fisher, J. C.; Tanthana, J.; Chuang, S. S. C., Oxide-supported tetraethylenepentamine for CO2 capture. *Environmental Progress & Sustainable Energy* **2009,** *28* (4), 589-598.
18. Jo, D. H.; Jung, H.; Shin, D. K.; Lee, C. H.; Kim, S. H., Effect of amine structure on CO2 adsorption over tetraethylenepentamine impregnated poly methyl methacrylate supports. *Separation and Purification Technology* **2014,** *125*, 187-193.
19. Hicks, J. C.; Drese, J. H.; Fauth, D. J.; Gray, M. L.; Qi, G.; Jones, C. W., Designing Adsorbents for CO2 Capture from Flue Gas-Hyperbranched Aminosilicas Capable of Capturing CO2 Reversibly. *Journal of the American Chemical Society* **2008,** *130* (10), 2902-2903.
20. Koutsianos, A.; Barron, A. R.; Andreoli, E., CO2 Capture Partner Molecules in Highly Loaded PEI Sorbents. *The Journal of Physical Chemistry C* **2017,** *121* (39), 21772-21781.
21. Andreoli , E.; Barron , A. R., Activation Effect of Fullerene C60 on the Carbon Dioxide Absorption Performance of Amine-Rich Polypropylenimine Dendrimers. *ChemSusChem* **2015,** *8* (16), 2635-2644.
22. Andreoli, E.; Barron, A. R., Effect of spray-drying and cryo-milling on the CO2 absorption performance of C60 cross-linked polyethyleneimine. *Journal of Materials Chemistry A* **2015,** *3* (8), 4323-4329.
23. Andreoli, E.; Cullum, L.; Barron, A. R., Carbon Dioxide Absorption by Polyethylenimine-Functionalized Nanocarbons: A Kinetic Study. *Industrial & Engineering Chemistry Research* **2015,** *54* (3), 878-889.
24. Andreoli, E.; Barron, A. R., Correlating Carbon Dioxide Capture and Chemical Changes in Pyrolyzed Polyethylenimine-C60. *Energy & Fuels* **2015,** *29* (7), 4479-4487.
25. Andreoli, E.; Dillon, E. P.; Cullum, L.; Alemany, L. B.; Barron, A. R., Cross-Linking Amine-Rich Compounds into High Performing Selective CO2 Absorbents. **2014,** *4*, 7304.
26. Hwang, K.-S.; Park, H.-Y.; Kim, J.-H.; Lee, J.-Y., Fully organic CO2 absorbent obtained by a Schiff base reaction between branched poly(ethyleneimine) and glutaraldehyde. *Korean Journal of Chemical Engineering* **2018,** *35* (3), 798-804.
27. Finzel, M. C.; Delong, J.; Hawley, M. C., Effect of stoichiometry and diffusion on an epoxy/amine reaction mechanism. *Journal of Polymer Science Part A: Polymer Chemistry* **1995,** *33* (4), 673-689.
28. Benyahya, S.; Aouf, C.; Caillol, S.; Boutevin, B.; Pascault, J. P.; Fulcrand, H., Functionalized green tea tannins as phenolic prepolymers for bio-based epoxy resins. *Industrial Crops and Products* **2014,** *53*, 296-307.
29. Lapique, F.; Redford, K., Curing effects on viscosity and mechanical properties of a commercial epoxy resin adhesive. *International Journal of Adhesion and Adhesives* **2002,** *22* (4), 337-346.
30. Ho, T.-H.; Wang, C.-S., Modification of epoxy resin with siloxane containing phenol aralkyl epoxy resin for electronic encapsulation application. *European Polymer Journal* **2001,** *37* (2), 267-274.
31. Fu, Y.-X.; He, Z.-X.; Mo, D.-C.; Lu, S.-S., Thermal conductivity enhancement with different fillers for epoxy resin adhesives. *Applied Thermal Engineering* **2014,** *66* (1), 493-498.
32. Jin, F.-L.; Li, X.; Park, S.-J., Synthesis and application of epoxy resins: A review. *Journal of Industrial and Engineering Chemistry* **2015,** *29*, 1-11.

33. Potter, W. G., *Uses of Epoxy Resins*. Newnes-Butterworths: London, 1975.
34. Rohde, B. J.; Robertson, M. L.; Krishnamoorti, R., Concurrent curing kinetics of an anhydride-cured epoxy resin and polydicyclopentadiene. *Polymer* **2015,** *69*, 204-214.
35. Vanlandingham, M. R.; Eduljee, R. F.; Gillespie Jr, J. W., Relationships between stoichiometry, microstructure, and properties for amine-cured epoxies. *Journal of Applied Polymer Science* **1999,** *71* (5), 699-712.
36. Bourne, L. B.; Milner, F. J. M.; Alberman, K. B., Health Problems of Epoxy Resins and Amine-curing Agents. *British Journal of Industrial Medicine* **1959,** *16* (2), 81-97.
37. Roudsari, G. M.; Mohanty, A. K.; Misra, M., Study of the curing kinetics of epoxy resins with biobased hardener and epoxidized soybean oil. *ACS Sustainable Chem. Eng* **2014,** *2*, 2111-2116.
38. Tan, Y.; Shao, Z.-B.; Yu, L.-X.; Xu, Y.-J.; Rao, W.-H.; Chen, L.; Wang, Y.-Z., Polyethyleneimine modified ammonium polyphosphate toward polyamine-hardener for epoxy resin: Thermal stability, flame retardance and smoke suppression. *Polymer Degradation and Stability* **2016,** *131*, 62-70.
39. Mao, X.; Shimai, S.; Wang, S., Gelcasting of alumina foams consolidated by epoxy resin. *Journal of the European Ceramic Society* **2008,** *28* (1), 217-222.
40. Kamae, T.; Drzal, L. T., Carbon fiber/epoxy composite property enhancement through incorporation of carbon nanotubes at the fiber–matrix interphase – Part I: The development of carbon nanotube coated carbon fibers and the evaluation of their adhesion. *Composites Part A: Applied Science and Manufacturing* **2012,** *43* (9), 1569-1577.
41. Li, P.; Zhang, S.; Chen, S.; Zhang, Q.; Pan, J.; Ge, B., Preparation and adsorption properties of polyethylenimine containing fibrous adsorbent for carbon dioxide capture. *Journal of Applied Polymer Science* **2008,** *108* (6), 3851-3858.
42. Jung, H.; Jeon, S.; Jo, D. H.; Huh, J.; Kim, S. H., Effect of crosslinking on the CO2 adsorption of polyethyleneimine-impregnated sorbents. *Chemical Engineering Journal* **2017,** *307*, 836-844.
43. Kang, J.; Wang, C.; Li, D.; He, G.; Tan, H., Nanoscale crosslinking in thermoset polymers: a molecular dynamics study. *Physical Chemistry Chemical Physics* **2015,** *17* (25), 16519-16524.
44. Gao, F.; Li, Y.; Bian, Z.; Hu, J.; Liu, H., Dynamic hydrophobic hindrance effect of zeolite@zeolitic imidazolate framework composites for CO2 capture in the presence of water. *Journal of Materials Chemistry A* **2015,** *3* (15), 8091-8097.
45. Nguyen, J. G.; Cohen, S. M., Moisture-Resistant and Superhydrophobic Metal−Organic Frameworks Obtained via Postsynthetic Modification. *Journal of the American Chemical Society* **2010,** *132* (13), 4560-4561.
46. Huang, H. Y.; Yang, R. T.; Chinn, D.; Munson, C. L., Amine-Grafted MCM-48 and Silica Xerogel as Superior Sorbents for Acidic Gas Removal from Natural Gas. *Industrial & Engineering Chemistry Research* **2003,** *42* (12), 2427-2433.
47. Franchi, R. S.; Harlick, P. J. E.; Sayari, A., Applications of Pore-Expanded Mesoporous Silica. 2. Development of a High-Capacity, Water-Tolerant Adsorbent for CO2. *Industrial & Engineering Chemistry Research* **2005,** *44* (21), 8007-8013.
48. Loganathan, S.; Ghoshal, A. K., Amine tethered pore-expanded MCM-41: A promising adsorbent for CO2 capture. *Chemical Engineering Journal* **2017,** *308*, 827-839.
49. Yue, M. B.; Chun, Y.; Cao, Y.; Dong, X.; Zhu, J. H., CO2 Capture by As-Prepared SBA-15 with an Occluded Organic Template. *Advanced Functional Materials* **2006,** *16* (13), 1717-1722.
50. Heydari-Gorji, A.; Sayari, A., CO2 capture on polyethylenimine-impregnated hydrophobic mesoporous silica: Experimental and kinetic modeling. *Chemical Engineering Journal* **2011,** *173* (1), 72-79.
51. McDonald, T. M.; Mason, J. A.; Kong, X.; Bloch, E. D.; Gygi, D.; Dani, A.; Crocellà, V.; Giordanino, F.; Odoh, S. O.; Drisdell, W. S.; Vlaisavljevich, B.; Dzubak, A. L.; Poloni, R.; Schnell, S. K.; Planas, N.; Lee, K.; Pascal, T.; Wan, L. F.; Prendergast, D.; Neaton, J. B.; Smit, B.; Kortright, J. B.; Gagliardi, L.; Bordiga, S.; Reimer, J. A.; Long, J. R., Cooperative insertion of CO2 in diamine-appended metal-organic frameworks. *Nature* **2015,** *519*, 303.
52. Liao, P.-Q.; Chen, H.; Zhou, D.-D.; Liu, S.-Y.; He, C.-T.; Rui, Z.; Ji, H.; Zhang, J.-P.; Chen, X.-M., Monodentate hydroxide as a super strong yet reversible active site for CO2 capture from high-humidity flue gas. *Energy & Environmental Science* **2015,** *8* (3), 1011-1016.
53. Park, S. E.; Chang, J. S.; Lee, K. W., *Carbon Dioxide Utilization for Global Sustainability: Proceedings of the 7th International Conference on Carbon Dioxide Utilization, Seoul, Korea, October 12-16, 2003*. Elsevier Science: 2004.
54. Granite, E. J.; Pennline, H. W., Photochemical Removal of Mercury from Flue Gas. *Industrial & Engineering Chemistry Research* **2002,** *41* (22), 5470-5476.
55. Socrates, G., *Infrared and Raman Characteristic Group Frequencies: Tables and Charts*. Wiley: 2001.
56. Walton, K. S.; Sholl, D. S., Predicting multicomponent adsorption: 50 years of the ideal adsorbed solution theory. *AIChE Journal* **2015,** *61* (9), 2757-2762.
57. Hahn, M. W.; Jelic, J.; Berger, E.; Reuter, K.; Jentys, A.; Lercher, J. A., Role of Amine Functionality for CO2 Chemisorption on Silica. *The Journal of Physical Chemistry B* **2016,** *120* (8), 1988-1995.
58. Goeppert, A.; Zhang, H.; Sen, R.; Dang, H.; Prakash, G. K. S., Oxidation-Resistant, Cost-Effective Epoxide-Modified Polyamine Adsorbents for CO2 Capture from Various Sources Including Air. *ChemSusChem* **2019,** *12* (8), 1712-1723.

SYNOPSIS TOC